

Numerical Significance of Brownian motion and activation energy on Cassonnanofluid involving gyrotactic microorganisms with Local thermal non-equilibrium effects in a porous medium.

Dyapa Hymavathi

Assistant Professor, Department of Mathematics, University college of Science, Mahatma Gandhi University, Nalgonda, Telangana, India, 508254

Abstract:

With the aid of Matlab software, the effects of Brownian motion and thermophoresis Over a stretching sheet through a porous media, stable, incompressible, laminar flows of Cassonnanofluid have been investigated. For both solids and liquids, separate thermal conservative equations are generated with an effect of local thermal non-equilibrium conditions, and the momentum equations are also formulated. These higher-order nonlinear derivatives are derived from an ODE system. With the aid of BVP5c approach, the impacted parameters are graphically analysed in depth. Also, the behaviour of the momentum equations' boundary layer is explored.

Keywords: Activation Energy, non equilibrium condition, Brownian motion, thermophoresis, Casson fluid, bio-convection.

Introduction:

The majority of research has focused on non-Newtonian nanofluids due to their versatility in modern high-technology industries such as extrusion of molten polymers, food processing, and fibre and wire coating. One of the most prevalent non-Newtonian fluid kinds is Casson fluid. Casson fluids are the result of research into non Newtonian liquids with convectional Cauchy stress. With divergent geometrical conditions, the Casson fluid with nanoparticles becomes more attractive. The behaviour of Casson fluid has recently been elucidated for physicochemical parameters having effects of thermophoresis and Brownian motion include Sherwood number, Nusselt number and skin friction coefficient [1]–[3].

To model the transformation of heat in porous medium, two models are available. The first model takes into account the local thermal equilibrium (LTE) between the liquid component and the solid component structures in order to resolve the energy equation in the medium which is porous. The LTE between solid structure and liquidstructure is disregarded in the second model. The porous equations are two separate thermal energycalculations are used to treatboth the liquid component and the solid component phases to represent convective heat transfer. The LTE approach is valid for modest heat differences between liquid component and the solid component phases in a permeable zone. The LTNE approach is necessary when variances in temperature are large and the LTE condition is not true in particular applications. When employing the LTNE model, yet another temperature boundary restriction needs to be specified at the boundary. First two field models for the thermal energy equations were developed by Nield and Benjan[4]. Instead of using a single equation of energy for the solid and liquid phases, they employed two separate equations. In order to study the flow of a fluid through porous medium, Malashetty et al. [5] established an LTNE model that

combined the Lapwood-Brinkman and two-field models. Recently, some studies [6]–[8] and [9] revealed that the numerical results and physical influenced parameters effects on Under various geometrical circumstances, the transfer of heat and mass occurs for the condition of the local heat non-equilibrium motion of non-Newtonian fluids, For rising values of the thermophoresis parameter and Brownian motion studies using the Jeffery fluid, for example, demonstrate that greater fluid phase heat transfer than Oldroyd-B liquid decreases the liquid and solid phase heat trajectories. Species chemical interactions with finite Arrhenius activation energies are a key criteria that is infrequently observed in natural convective boundary layer flows with simultaneous heat and mass transport. Tencer[10] is the most common form of the Arrhenius equation. $K = B \left(\frac{T}{T_\infty}\right)^n \exp\left(\frac{-E_a}{kT}\right)$ where B is the preexponential factor, while K is the rate constant for chemical reactions. Prefactor is based on the simple observation that reactions accelerate noticeably when the temperature is raised often. The Boltzmann constant, $k = 8.61 \times 10^{-5} \text{ eV}/K$, is a physical constant that links energy at the level of a single particle with temperature observed at a collective or bulk level. E_a represents the activation energy. The previous phenomenon is usually applicable in areas such as geothermal or oil reservoir engineering. Aside from experimental work in these areas, It is also required to make theoretical attempts to forecast the outcomes of the activation energy in the aforementioned flows. However, the literature in this area contains extremely few theoretical papers. This is due to the system's chemical reaction pathways being highly complicated, which also causes the mass transfer equations necessary for all of the reactions to become quite complex. In theory, Solving such an equation is essentially impossible. This is a highly challenging topic from the perspective of chemical kinetics, but if the reaction is limited to binary type, great progress can be made. Bestman[11] explored a straightforward binary reaction model and made the assumption that there would be substantial motion through the plate, which enabled him to derive analytical solutions for a range of activation energy values. In his study, In the presence of thermal radiation, Abdul Maleque[12] looked into the impact of endothermic/exothermic reactions with Arrhenius activation energy of mass transfer flow. Muhammad Ijaz Khan [13] investigated the impact of activation energy in nonlinear radiative conditions at the stagnation point flow of Cross nanoliquid. One of the most well-known eras in bioscience is the phenomenon of bioconvection. This phenomenon is caused by the upwardly average swimming of microorganisms that are denser than a base fluid such as water. When the suspension is exceedingly dense, microorganism aggregation causes the suspension's upper surface to become unstable, which causes bioconvection currents to form and microorganisms to tumble. In the presence of gyrotactic microorganisms, Kuzntsov[14] described the bioconvection of nanoparticles over a conduction heated horizontal plate. Kuznestov and Avramenko[15] investigated the bioconvection phenomenon using a suspension of gyrotactic microorganisms. The effects of gyrotactic microorganisms in a continuous flow of magneto- Burgers nanofluid were studied by Khan et al. [16]. Begum et al [17] attempted to investigate the numerical results of Stefan blowing and multiple slip effects of gyrotactic microorganisms suspended in nanoparticles through saturated porous media. M. J Uddin et al [18] investigated the numerical results of Stefan blowing and multiple slip effects of gyrotactic microorganisms suspended in nanoparticles through saturated porous media. Qiu- Hong Shi et al. [19] and Hassan Waqas et al. [20] recently investigated the effect of activation energy on gyrotactic microorganisms in nanoparticles with magneto Crossed and Maxwell fluids.

After all these reviews the main purpose of this assumption of Cassonnanoliquid's heat and mass transfer in porous media with an effect of Activation energy and non equilibrium thermal transport over a stretching sheet is to investigate the behavior of physical parameters for temperature, velocity, and concentration of dimensionless fluids of Cassonnanoliquid and density of motile microorganisms also the validation of the other

physical influenced parameters such as Sherwood number, Nusselt number, skin friction coefficient, and rate of motile microorganisms motion are achieved with the help of BVP5c technique along with Matlab software. The significant outcomes for the separate models Non equilibrium thermal transport for fluid and solids are discussed in detailed. And the present assumption analysis is played an important role in creation of industrial manufacturing systems with nano-biomaterials where the thermal transport process is involved

Mathematical bio- nano-liquid Formulation:

The research considers a sheet stretched at the velocity $U_w = cx$ in a porous medium with a continuous incompressible laminar flow of Casson liquid involving gyrotactic bioconvection boundary layer flow. The flow is being constrained to $y > 0$ and occurring on $y = 0$. Moreover, it is anticipated that the perpendicular to the sheet applied magnetic B_0 will be present. Also, when Sd effects occur, the mechanics of mass and heat movement are taken into account. It is believed that the porous medium is homogenous. To examine how much heat is transferred between the solid and liquid phases, two different heat transport equations are used. Let v_w stand for the mass transfer-induced surface blowing velocity that is proportionate to the flux of mass transfer at the sheet's surface. The mass transfer flux at the sheet's surface will determine the sheet's surface blowing velocity. It is believed that the nanofluid is constant in flow and contains gyrotactic bacteria. Additionally, it is presumable that the nanoparticle suspension is stable and that nanoparticles have no bearing on the direction in which microorganisms swim. The surface-level temperature, nanoparticle volume fraction, and motile microbe density are specified as T_w, C_w, n_w respectively, where T_∞, C_∞, n_w signify their ambient values. The energy equation under this assumption ignores viscous dissipation. According to [9] and [19], the passive boundary conditions taken into account to conserve mass, momentum, thermal energy, nanoparticles, and microorganisms

$$\frac{\partial u}{\partial x} + \frac{\partial v}{\partial y} = 0, \tag{1}$$

$$\frac{1}{\varepsilon^2} \left[u \frac{\partial u}{\partial x} + v \frac{\partial u}{\partial y} \right] = \frac{\mu_f}{\rho_f} \left(1 + \frac{1}{\beta} \right) \left(\frac{\partial^2 u}{\partial y^2} + \frac{\partial^2 u}{\partial x^2} \right) - \frac{\mu_f}{\rho_f K^*} u - \frac{\sigma_f B_0^2}{\rho_f} u, \tag{2}$$

$$\frac{1}{\varepsilon} \left[u \frac{\partial T_f}{\partial x} + v \frac{\partial T_f}{\partial y} \right] = \frac{k_f}{(\rho C_p)_f} \left(\frac{\partial^2 T_f}{\partial y^2} + \frac{\partial^2 T_f}{\partial x^2} \right) + \frac{16\sigma T_\infty^3}{3k^*(\rho C)_f} \frac{\partial^2 T_f}{\partial y^2} + \frac{h_{fs}}{\varepsilon(\rho C_p)_f} (T_s - T_f) + \frac{(\rho c)_p}{(\rho c)_f} \left(D_B \frac{\partial C}{\partial y} \frac{\partial T_f}{\partial y} + \frac{D T_f}{T_\infty} \left(\frac{\partial T_f}{\partial y} \right)^2 \right), \tag{3}$$

$$0 = \frac{k_s}{(\rho C_p)_s} \left(\frac{\partial^2 T_s}{\partial y^2} + \frac{\partial^2 T_s}{\partial x^2} \right) + \frac{h_{fs}}{(1-\varepsilon)(\rho C_p)_s} (T_f - T_s) + \frac{(\rho c)_p}{(\rho c)_f} \left(D_B \frac{\partial C}{\partial y} \frac{\partial T_s}{\partial y} + \frac{D T_s}{T_\infty} \left(\frac{\partial T_s}{\partial y} \right)^2 \right), \tag{4}$$

$$\frac{1}{\varepsilon} \left[u \frac{\partial C}{\partial x} + v \frac{\partial C}{\partial y} \right] = D_m \left(\frac{\partial^2 C}{\partial y^2} + \frac{\partial^2 C}{\partial x^2} \right) + \frac{D_m k_T}{T_m} \frac{\partial^2 T_f}{\partial y^2} - k_c^2 (C - C_\infty) \left(\frac{T}{T_\infty} \right)^n \exp \left(-\frac{E_a}{kT} \right), \tag{5}$$

$$\frac{1}{\varepsilon} \left[u \frac{\partial n}{\partial x} + v \frac{\partial n}{\partial y} \right] + \frac{bW_c}{(C_w - C_\infty)} \left[\frac{\partial}{\partial y} \left(n \frac{\partial C}{\partial y} \right) \right] = D_m \left(\frac{\partial^2 n}{\partial y^2} \right), \tag{6}$$

Where g is the gravitational constant, ρ is the density of nanoparticles, E_a is activation energy, the motility of microorganisms is measured by n , which is also the Arrhenius expression, σ_s is the Stefan- Boltzmann constant, reaction rate k_c, k^* mean absorption coefficient. Eq.(1) is the continuity equation, by the momentum conservation rule Eq. (2) is die momentum- equation. Inertial forces are responsible for the primary factor on the left side of Eq. (2), whereas that final and preceding term is caused by the additional influence of porous media and the magnetic field. Eq. (3) states that heat can be transferred through a fluid by convection (LHS),

through conduction as the first term on the RHS, and through heat exchanges between solid and liquid phases as the second term. The kind of porous matrix and saturating fluid determine the h_{fs} and its value has drawn a lot of experimental attention. Rapid heat transfer between the phases is brought on by high h_{fs} values. Eq. (5) denotes the mass diffusion equation, where the last term of RHS is the Arrhenius expression with activation energy. While Eq. (6) represents the condervation of motile microorganisms density.

The following are the definitions of passive boundary conditions:

$$\left. \begin{aligned} u = cx, v = v_w, T_f = T_w, T_p = T_w, C = C_w \text{ at } y = 0, \\ u \rightarrow 0, T_f \rightarrow T_\infty, T_p \rightarrow T_\infty, C \rightarrow C_\infty \text{ as } y \rightarrow \infty \end{aligned} \right\} \quad (7)$$

The stream function is stated as follows:

$$\Psi = \sqrt{cv_f} x f(\eta), \eta = \sqrt{\frac{c}{v_f}} y, u = cx f', v = -\sqrt{cv_f} f$$

$$\theta_f(\eta) = \frac{T_f - T_\infty}{T_w - T_\infty}, \theta_s(\eta) = \frac{T_s - T_\infty}{T_w - T_\infty}, \phi(\eta) = \frac{C - C_\infty}{C_w - C_\infty}, g(\eta) = \frac{n - n_\infty}{n_w - n_\infty}$$

These defined functions are used to convert the controlled equations (2)–(6) and boundary conditions into ordinary differential equations, as shown below.

$$\left(1 + \frac{1}{\beta}\right) f''' - \frac{1}{\varepsilon^2} [f'^2 - f f''] - K f' - M f' = 0, \quad (8)$$

$$\frac{1}{Pr} \theta''_f + \frac{1}{\varepsilon} f \theta'_f + H(\theta_s - \theta_f) + Nb \theta' \phi' + Nt \theta'^2 = 0 \quad (9)$$

$$\frac{1}{Pr} \theta''_s + \gamma H(\theta_f - \theta_s) + Nb \theta' \phi' + Nt \theta'^2 = 0, \quad (10)$$

$$\frac{1}{Sc} \phi'' + \frac{1}{\varepsilon} f \phi' + \frac{Nt}{Nb} \theta'' - \sigma(1 + \delta \theta)^n \exp\left(-\frac{E}{1 + \delta \theta}\right) = 0, \quad (11)$$

$$\frac{1}{Lb} g'' + \frac{1}{\varepsilon} f g' - Pe[g' \phi' + (g + \Omega) \phi''] = 0 \quad (12)$$

The similarity transformations' lowered boundary conditions

$$\left. \begin{aligned} f'(0) = 1, f(0) = k1 \phi'(0), \theta_f(0) = 1, \theta_s(0) = 1, \phi(0) = 1, g(0) = 1 \\ f'(\infty) \rightarrow 0, \theta_f(\infty) \rightarrow 0, \theta_s(\infty) \rightarrow 0, \phi(\infty) \rightarrow 0, g(\infty) \rightarrow 0 \end{aligned} \right\} \quad (13)$$

$K1$ is the mass transfer blowing parameter, and a wall's blowing velocity is determined by

$$v_w = -K \sqrt{cv_f} \phi'(0)$$

$$K = \frac{v_f}{ck^*}, M = \frac{\sigma_f B_0^2}{c \rho_f}, Pr = \frac{v_f}{\alpha_f}, H = \frac{h_{fs} \alpha_f}{\varepsilon k_f c}, Nb = \frac{\rho c_f D_B}{\nu \rho c_p} (C_w - C_\infty), Nt = \frac{\rho c_p D_T}{\rho c_f T_\infty \nu} (T_w - T_\infty),$$

$$\gamma = \frac{\varepsilon K}{(1 - \varepsilon) k_s}, Sc = \frac{v_f}{D_m}, \sigma = \frac{k_c^2}{c}, \delta = \frac{T_f - T_\infty}{T_\infty}, E = \frac{E_a}{k T_\infty}, Lb = \frac{v_f}{D_n}, Pe = \frac{b W_c}{v_f}, \Omega = \frac{n_\infty}{n_w - n_\infty}.$$

The quantities for physical interest:

The resistance to flow, rate of mass transfer and heat transfer are computed using the local Sherwood number, Nusselt number, skin friction relations. These relations, in their non-dimensional version, have a distinct structure:

$$\sqrt{Re}C_f = 2 \left(1 + \frac{1}{\beta}\right) f''(0), \frac{Nu_f}{\sqrt{Re}} = -\theta'_f(0), \frac{Nu_s}{\sqrt{Re}} = -\theta'_s(0), \frac{Sh}{\sqrt{Re}} = -\phi'(0), \frac{Nun}{\sqrt{Re}} = -g'(0)$$

Methodology:

To investigate the liquid model for the boundary conditions that go along with the ordinary differential equations (8) to (12). Eq. (13) for a variety of suitable parameter values $M, K, Pr, Nb, Nt, H, \gamma, Sc, \sigma, \delta, E, Lb, Pe, \Omega$ implementing the BVP5c methodology with Matlab program is used. Outlines of methodology is as follows,

$$f = f(1), f' = f(2), f'' = f(3), \theta_f = f(4), \theta'_f = f(5), \theta_s = f(6), \theta'_s = f(7), \phi = f(8), \phi' = f(9), g = f(10), g' = f(11),$$

The boundary value problems, which were composed of a system of equations, were then converted into initial value problems.

$$f'(3) = \left(1 + \frac{1}{\beta}\right) \left[\frac{1}{\epsilon^2} (f(2)f(2) - f(1)f(3)) + Kf(2) + Mf(2)\right],$$

$$f'(5) = -Pr \left[\frac{1}{\epsilon} f(1)f(5) + H(f(6) - f(4)) + Nbf(9)f(5) + Ntf(5)f(5)\right],$$

$$f'(7) = -Pr[\gamma H(f(4) - f(6)) + Nbf(9)f(5) + Ntf(5)f(5)],$$

$$f'(9) = -Sc \left[\frac{1}{\epsilon} f(1)f(9) + \frac{Nt}{Nb} f'(5) - \sigma(1 + \delta f(4))^n \exp\left(-\frac{E}{1 + \delta f(4)}\right)\right],$$

$$f'(11) = -Lb \left[\frac{1}{\epsilon} f(1)f(11) - Pe(f(11)f(9) + [f(10) + \Omega]f'(9))\right],$$

Initial and Boundary conditions for the proposed system in the BVP5c technique are defined as

$$fa(2) = 1, fa(1) = kfa(9), fa(4) = 1, fa(6) = 1, fa(8) = 1, fa(10) = 1,$$

$$fb(2) = 0, fb(4) = 0, fb(6) = 0, fb(8) = 0, fb(10) = 0 \text{ respectively.}$$

Results and Discussion:

The primary objective of the problem in this section aim to illustrate computational investigations and behaviour for the velocity, temperature, solubility, and motility profiles of microorganisms for a classification of non-dimensional physicochemical characteristics $M, K, Pr, Nb, Nt, H, \gamma, Sc, \sigma, \delta, E, Lb, Pe, \Omega$ and emerging from the problem. Gained system of highly nonlinear ordinary differential equations of second order in thermal, solutal, and motile microorganisms and third order in momentum for these

investigations. We used Matlab software and the Bvp5c technique is approached to achieve the numerical results of such a complex system.

The value of the coefficient of heat transfer and liquid viscosity both rise when the Casson fluid parameter increases. As the Casson parameter β is increased, the velocity field is impressed. The liquid acts like a Newtonian fluid when the Casson parameter β increases as its yield stress drops, as shown in figures 1(a)-1(e) f' upsurges and $\theta_f(\eta)$, $\theta_s(\eta)$, $\phi(\eta)$, $g(\eta)$ deteriorates. The fluid behaves as a Newtonian fluid as the yield stress decreases.

Figure 2(a) - 2(e) depicts the thickness of the momentum fluid layers as the magnetic field parameter M increases. The Lorentz force, which opposes the flow of fluid, is created as the magnetic field parameter M rises. This force causes the velocity boundary layer's thickness to decrease. According to this research, magnetic forces cause an additional layer of resistance to the stream, which slows it down and increases its temperature. The base liquid velocity field is retarded by the Lorentz force, and thermal energy is lost as a result of the additional energy needed to move the fluid in the direction of the magnetic field's action. This alerts the liquid to the rising temperature $\theta_f(\eta)$, $\theta_s(\eta)$, profile and concentration of Casson liquid and density of motile microorganism. Lower Prandtl number Pr results in higher thermal diffusivity, and as a result, heat transfer increases. The gradual thinning of the boundary layer characterises shear thickening activity. According to the definition, thermal diffusivity and Pr have an inverse relationship. As a result, the thermal profile rises while the density of motile microorganisms falls, as illustrated in Figures 3(a)-3 (c). The Prandtl number Pr denotes the relationship between momentum diffusivity and thermal diffusivity. The Brownian motion parameter influences heat transfer. Heat transfer rate enhancement varies from particle to particle due to differences in Brownian motion effect. Figures 4(a)-4(d) show that as the Brownian motion parameter Nb temperature raises, the concentration of nanoparticles and density of motile microorganisms increase, as does the thickness of the boundary layer. The activation energy is defined as the amount of excess energy transferred to the reactants during a chemical reaction. Physically, it is defined as the difference between the threshold energy and the molecule's average kinetic energy; higher activation energy results in a slower chemical reaction. Because of this, the productive chemical reaction causes the concentration of nanoparticles and density of microorganisms profiles to increase from figure 5(a)-5(e), while activation energy has no effect on velocity or temperature. Figure 6 clearly shows that at higher values of γ , temperature can be fully developed. Schmidt number Sc influences convection and characterises liquid flows. It is defined as the ratio of momentum diffusivity to mass diffusivity. Physical terms include the mass transport layer and the hydrodynamic thickness layer. The smaller Sc is correlated with increased nanoparticle concentration. Based on Figure 7(a)- 7(e), the thermal transport profile is decreasing, while the border layer's

nanoparticle concentration fluctuates between initially growing and falling. Figure 8 shows a perspective motile microorganisms profile for increasing values of bio convection Lewis number Lb . Lb is a dimensionless ratio of heat and mass diffusivity. With this behaviour, the density of motile microorganisms profile increases for a rising Lewis number as mass diffusivity increases. Smaller Peclet numbers increase wall heat flux, resulting in diffuse flow. Whereas a high Peclet number Pe depicts the advective flow distribution. As Pe decreases the wall, heat flux increases at the profiles of organisms, and as a result, Pe gradually decreases.

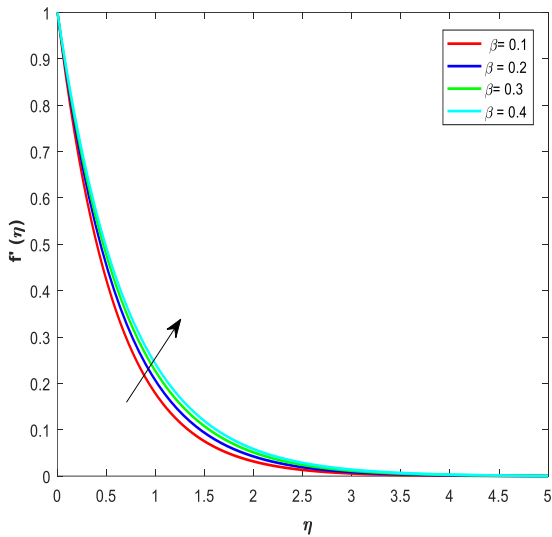


Figure 1(a)

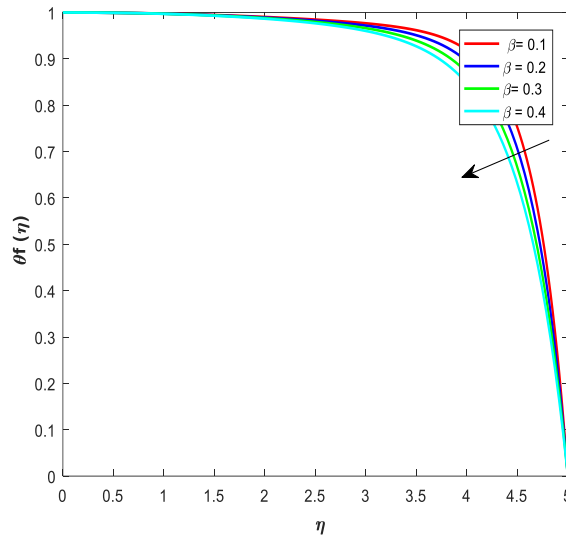


Figure 1(b)

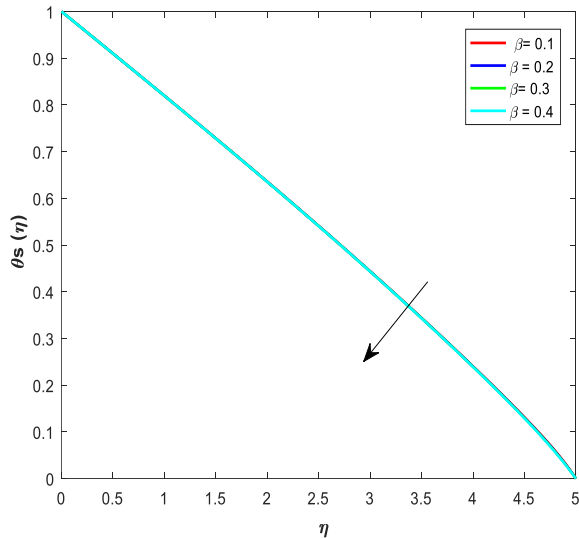


Figure 1(c)

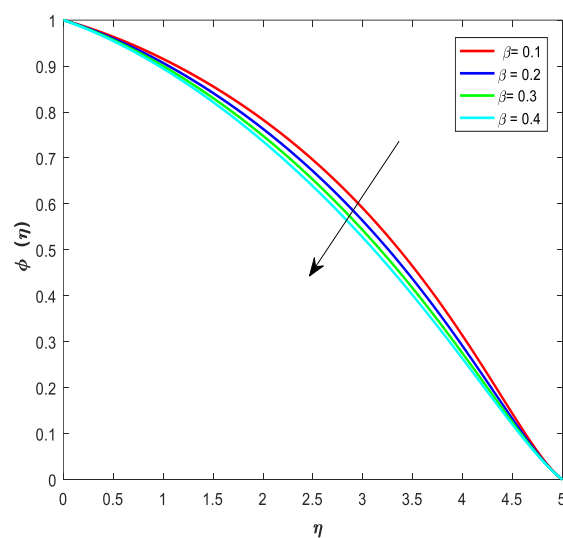


Figure 1(d)

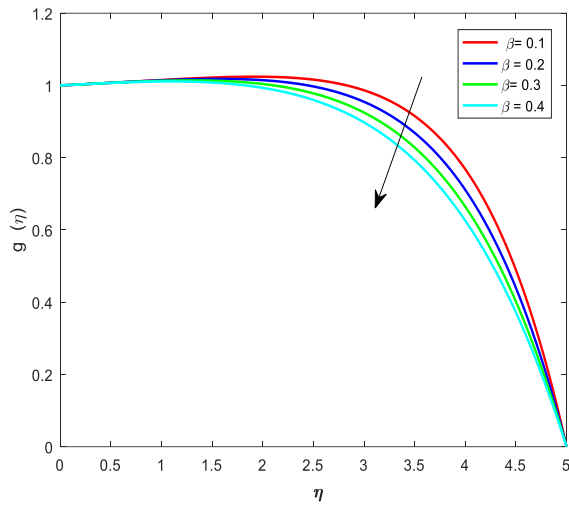


Figure 1(e)

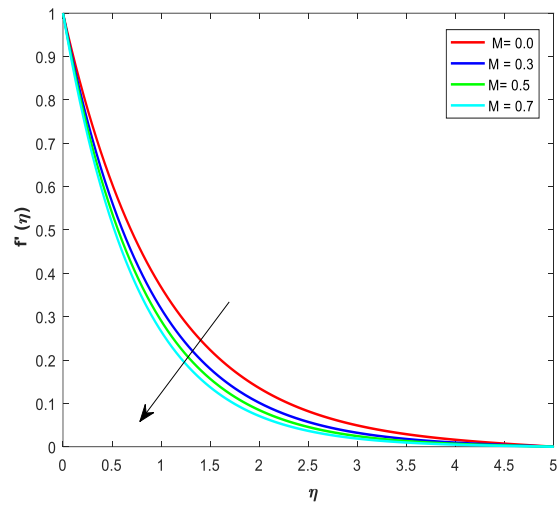


Figure 2(a)

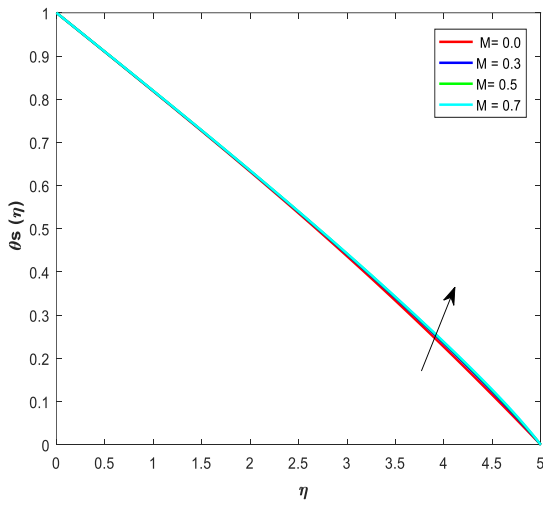


Figure 2(b)

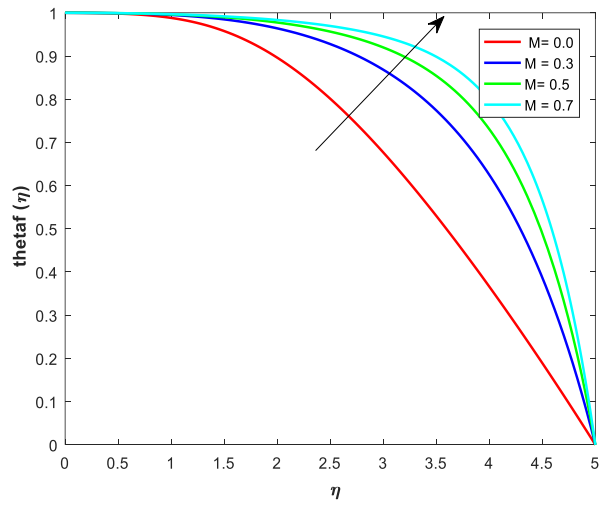


Figure 2(c)

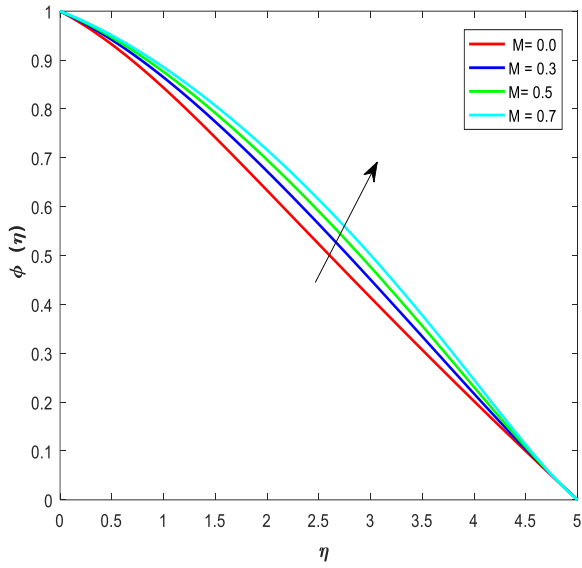


Figure 2(d)

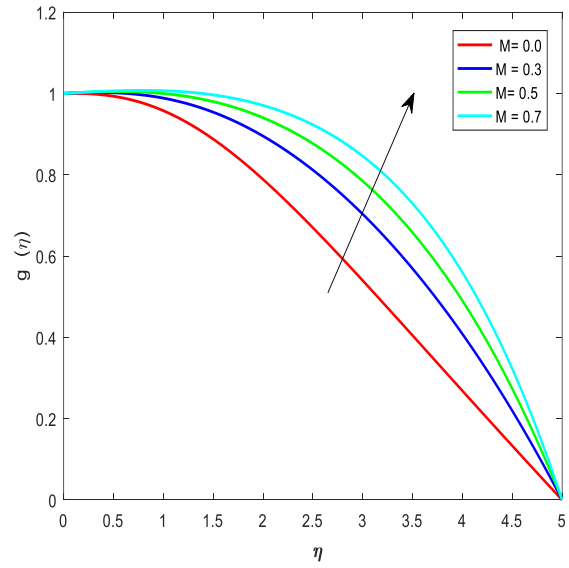


Figure 2(e)

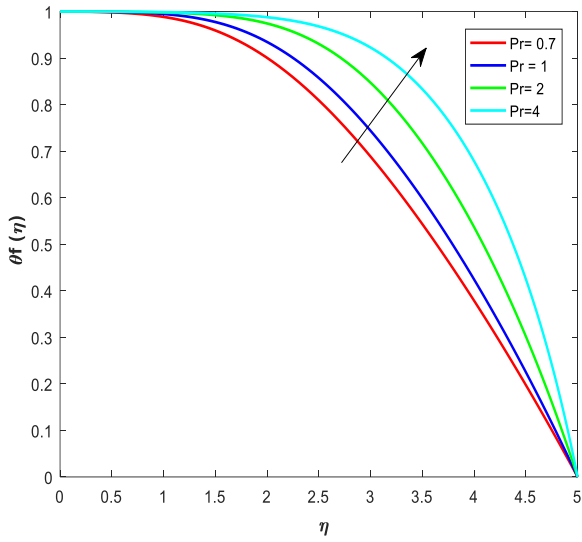


Figure 3(a)

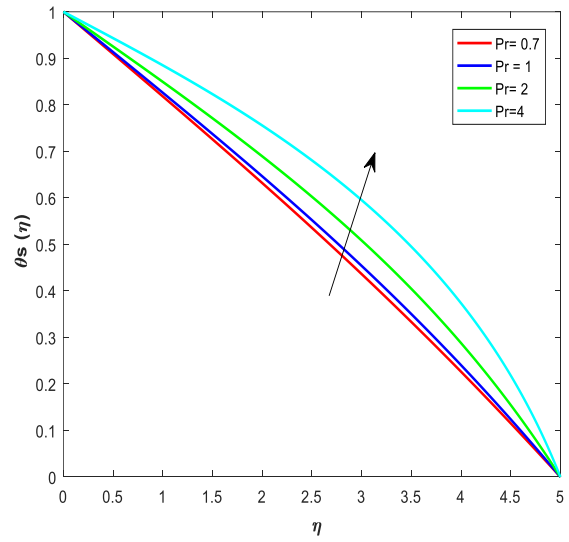


Figure 3(b)

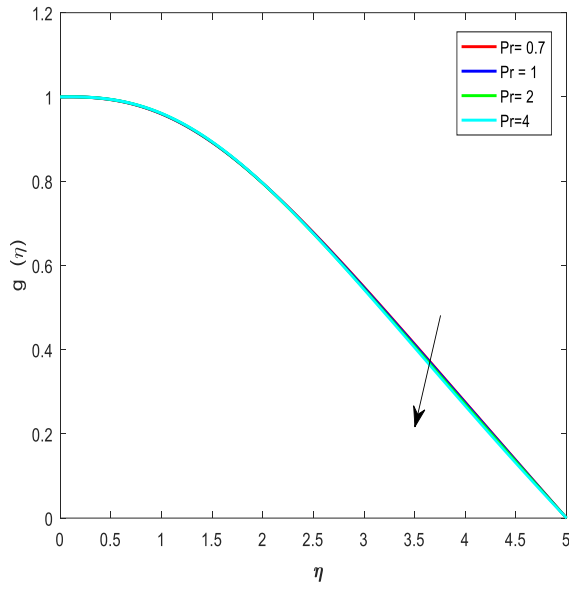


Figure 3(c)

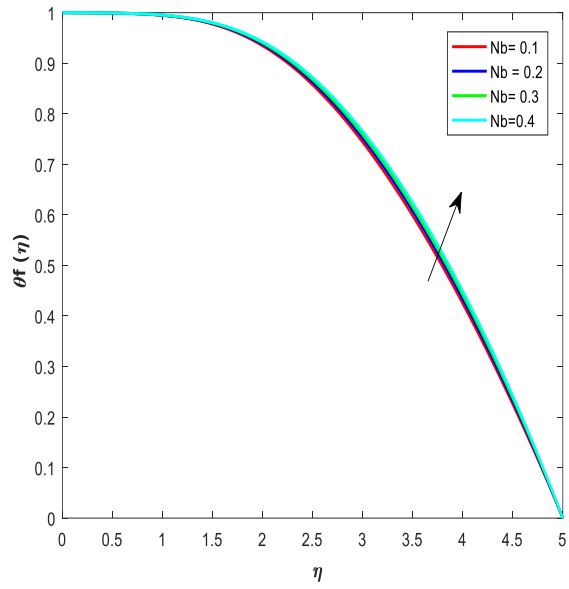


Figure 4(a)

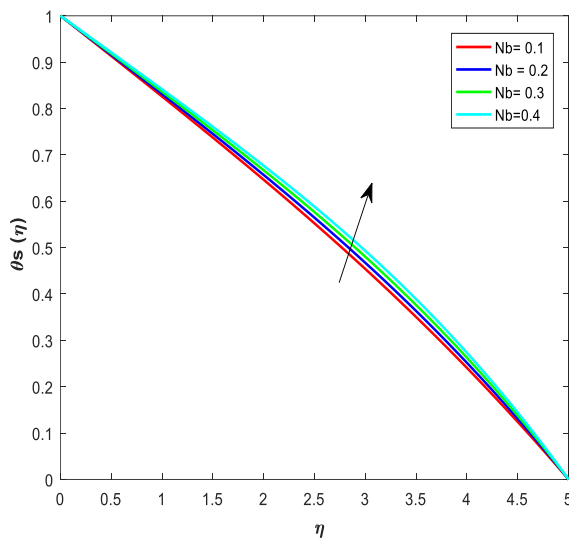


Figure 4(b)

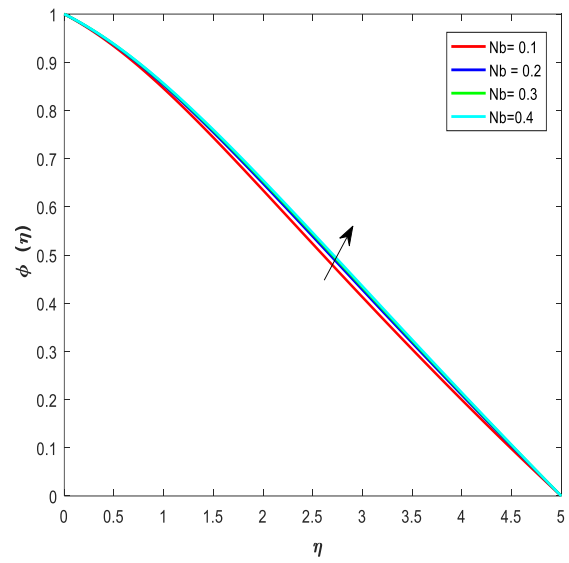


figure 4(c)

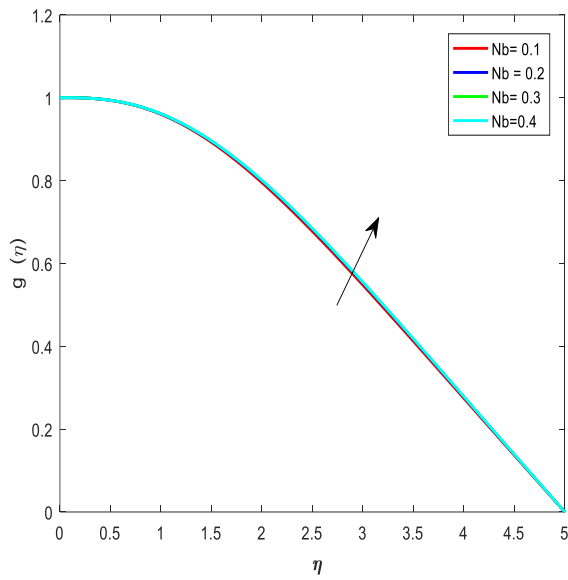


Figure 4(d)

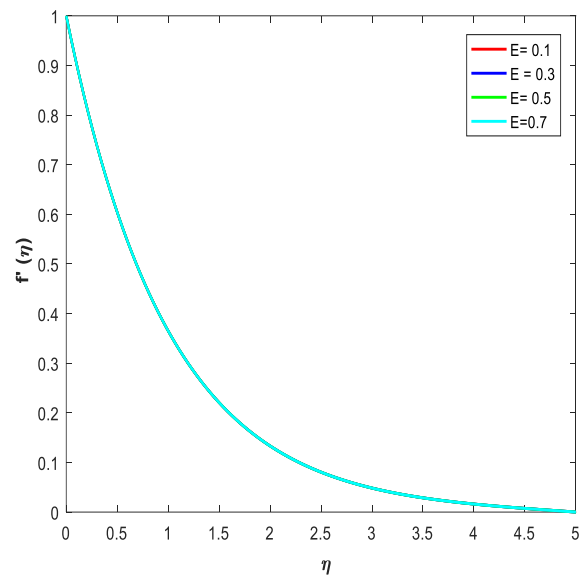


figure 5(a)

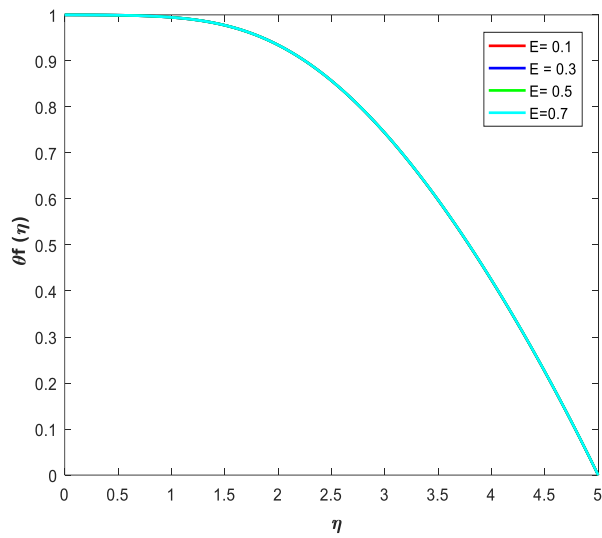


Figure 5(b)

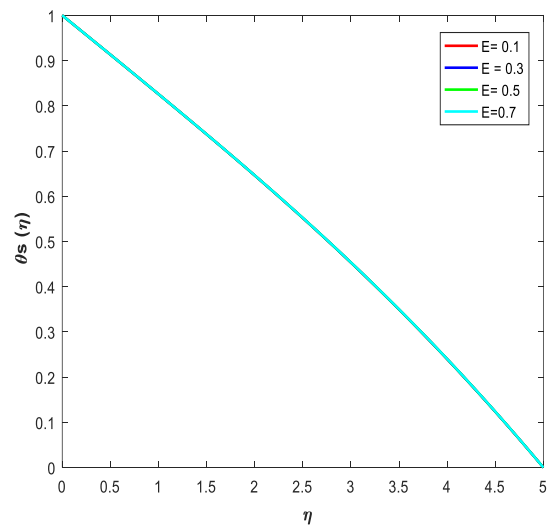


Figure 5(c)

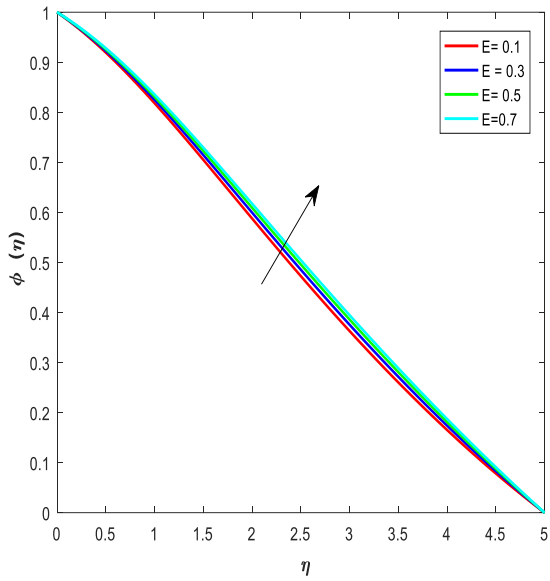


Figure 5(d)

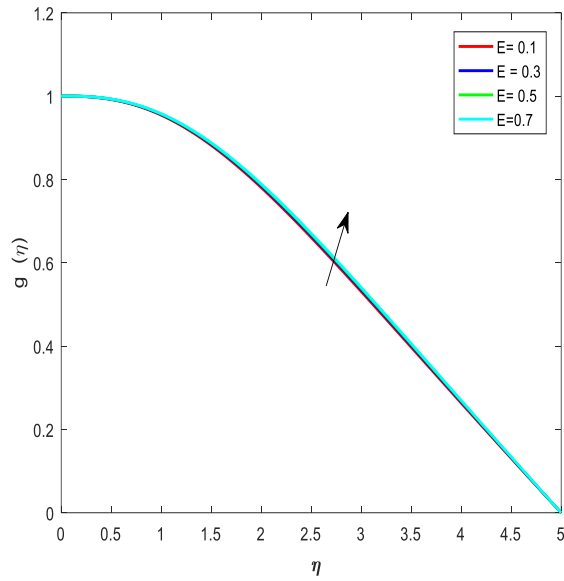


Figure 5(e)

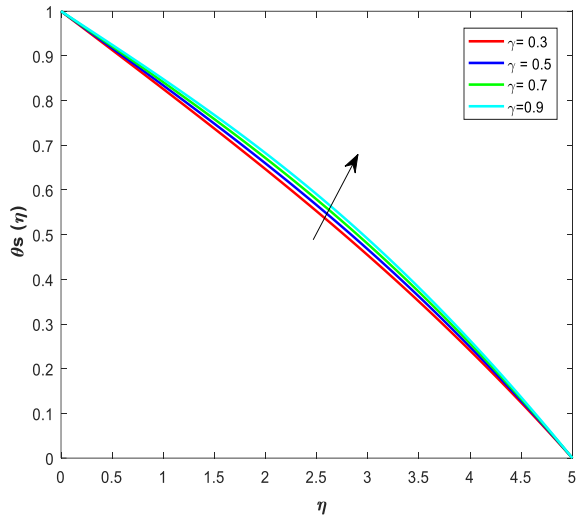


Figure 6

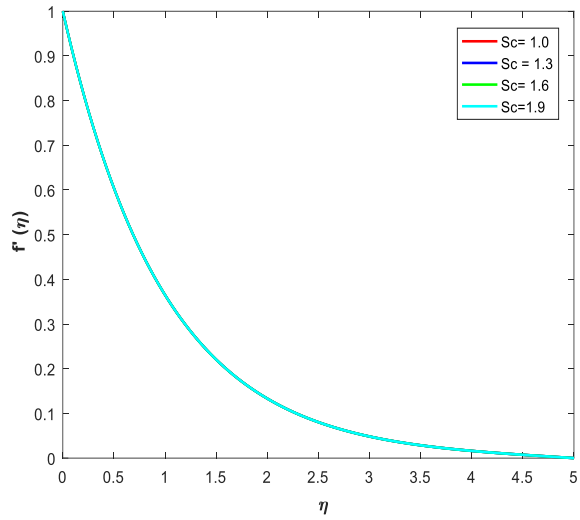


Figure 7(a)

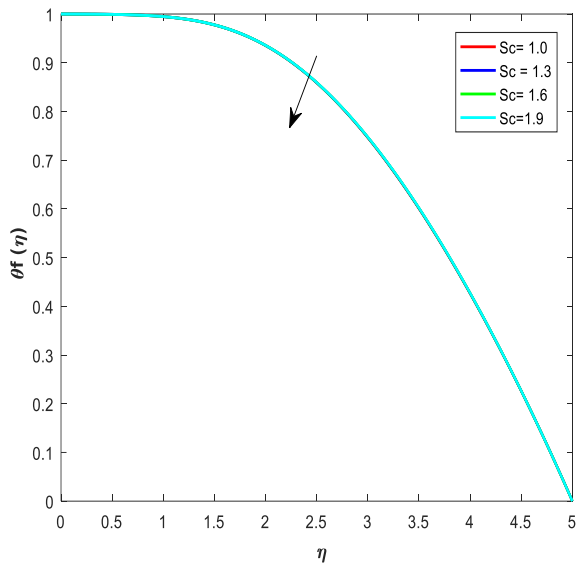


Figure 7(b)

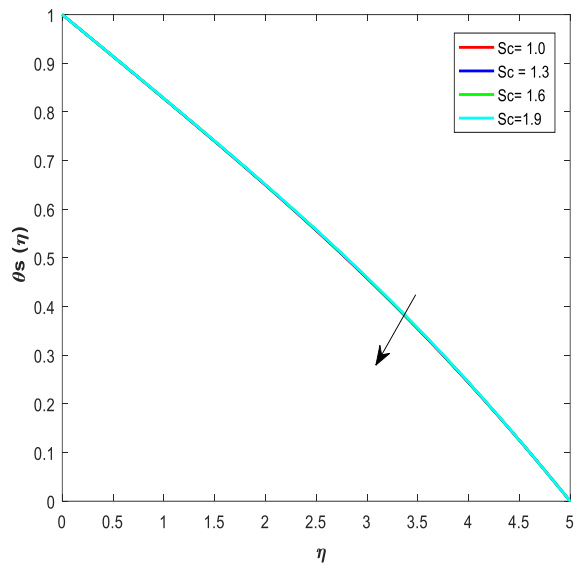


Figure 7(c)

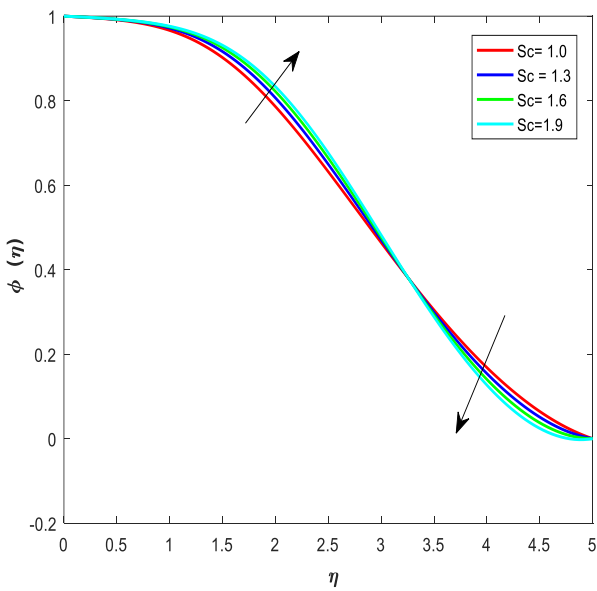


Figure 7(d)

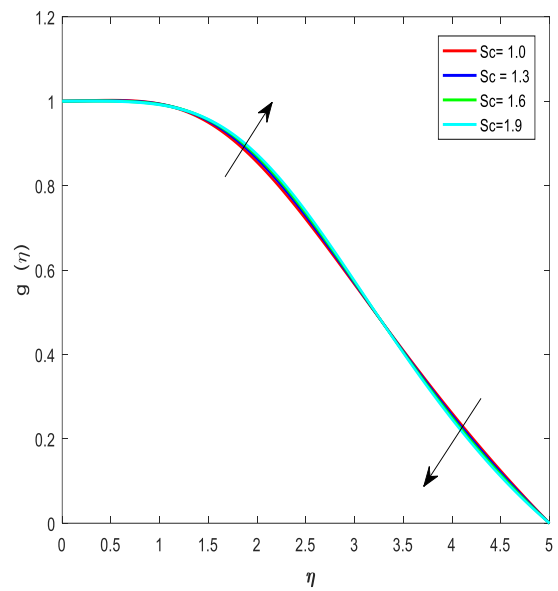


Figure7(e)

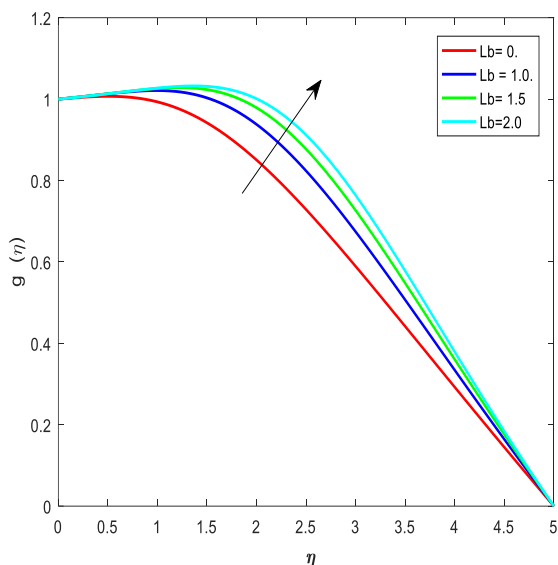


Figure 8

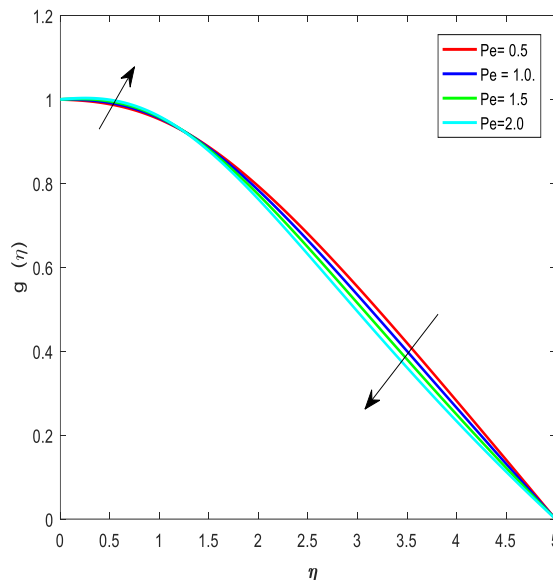


Figure 9

For the fixed values of physical parameter, Table 1-3 are shown the effects and changes in physical parameters

$\beta = 1.0; \varepsilon = 0.1; K = 0.5; Pr = 0.71; H = 0.1; Nb = 0.1; Nt = 0.1; \gamma = 0.3; Sc = 0.1; \sigma = 0.1; E = 0.1; \delta = 0.1; Lb = 0.3; Pe = 1.0; \Omega = 1.0; n = 1.0; ,$

Effects of physical parameters on physical significant fluid parameters Nusselt numbers for the solid phase and the fluid phase, Shearwood number and motile density rate of gyrotactic microorganisms and their behavior is clearly observed in these tables.

Table 1:

<i>M</i>	β	<i>K</i>	<i>Pr</i>	<i>Lb</i>	<i>Pe</i>	<i>Nu_f</i>	<i>Nu_s</i>	<i>Sh</i>	<i>Nu_n</i>
0.0						0.000790	0.181097	0.111890	-0.004133
0.3						0.000517	0.180418	0.096473	0.011138
0.5						0.000467	0.180121	0.088468	0.013166
0.7						0.000443	0.179941	0.081840	-0.014029
	0.1					0.000399	0.179626	0.060904	-0.012799
	0.2					0.000410	0.179692	0.066992	-0.013665
	0.3					0.000419	0.179758	0.071692	-0.014080
	0.4					0.000427	0.179814	0.075463	-0.014225
		0.0				0.000854	0.182281	0.113629	-0.003056
		0.1				0.000764	0.180999	0.109840	-0.004706
		0.2				0.000574	0.180634	0.100519	-0.009256
			0.7			0.000805	0.181277	0.109858	-0.004693
			1.0			0.000278	0.173165	0.109454	-0.004935
			2.0			0.000088	0.149184	0.108974	-0.005142
			4.0			0.000030	0.112848	0.108721	-0.005236
				0.5		0.000278	0.173274	0.130451	-0.020545
				1.0		0.000278	0.173274	0.130451	-0.023269
				1.5		0.000278	0.173274	0.130451	-0.022747
				2.0		0.000278	0.173271	0.130451	-0.022446
					0.5	0.000278	0.173274	0.130451	0.005227
					1.0	0.000278	0.173274	0.130451	-0.003994
					1.5	0.000278	0.173274	0.130451	-0.013226

				2.0	0.000278	0.173274	0.130451	-0.022458
--	--	--	--	-----	----------	----------	----------	-----------

Table 2:

Nb	Nt	Nu_f	Nu_s	Sh	Nu_n
0.1		0.000278	0.173165	0.109454	-0.004935
0.2		0.000268	0.167849	0.104543	-0.004485
0.3		0.000258	0.162686	0.102906	-0.004335
0.4		0.000248	0.157674	0.102088	-0.004260
	0.1	0.000278	0.173165	0.109454	-0.004935
	0.2	0.000268	0.167849	0.104543	-0.004485
	0.3	0.000258	0.162686	0.102906	-0.004335
	0.4	0.000248	0.157674	0.102088	-0.004260

Table 3:

δ	E	σ	Sc	γ	Nu_f	Nu_s	Sh	Nu_n
0.01					0.000278	0.173261	0.128415	-0.004113
0.03					0.000278	0.173262	0.128585	-0.004103
0.05					0.000278	0.173263	0.128750	-0.004093
0.07					0.000278	0.173264	0.128910	-0.004084
	0.1				0.000278	0.173298	0.135745	-0.003789
	0.3				0.000278	0.173265	0.129140	-0.004070
	0.5				0.000278	0.173238	0.123642	-0.004304
	0.7				0.000278	0.173215	0.119065	-0.004500
		0.1			0.000278	0.173165	0.109454	-0.004935
		0.3			0.000278	0.173298	0.135745	-0.003789
		0.5			0.000278	0.173431	0.162037	-0.002624
		0.7			0.000278	0.173563	0.188328	-0.001440
			1		0.000277	0.171696	0.010929	0.004721
			1.3		0.000276	0.171470	0.010413	-0.003190
			1.6		0.000276	0.171284	0.010172	-0.002299
			1.9		0.000276	0.171125	0.010027	-0.001729
				0.3	0.000278	0.173165	0.109454	-0.004935
				0.5	0.000265	0.164700	0.109444	-0.004941
				0.7	0.000254	0.156933	0.109435	-0.004947
				0.9	0.000243	0.149781	0.109426	-0.004952

Conclusions:

The emphasis of the current research is the heat and mass transfer of Cassonnanoliquid in porous media with the effect of activation energy and non-equilibrium thermal transport over a stretching sheet. The behavior of physical parameters on dimensionless fluid velocity, temperature, Cassonnanoliquid concentration, and motile microorganism density was also graphically analyzed using the BVP5c technique and Matlab software. The following are a few of the investigation's main findings:

- Brownian motion parameter and thermophoresis parameters are showing their impact as declined on Nusselt number of solid heat transfer rate when they are rising. While the fluid heat transfer rate Nusselt number does get impact with nano particles motion.
- When γ changes in positive mode Solid phase rate of heat transfer, rate of mass diffusivity and rate of density of motile microorganisms are declined, while fluid phase heat transfer is decreasing from $\gamma = 1$ to 1.5 and then it will be stable for remaining values of γ .
- Activating force E decreases the rate of transport of heat at solid phase and fluid phase, mass diffusion and microorganisms motion of Cassonnanofluids.
- For the improvement of δ Nusselt number for fluid phase is stable and solid phase and shearwood number are improved, while motile rate of microorganisms involving in Cassonnanoliquid is improving.

References:

- [1] W. A. Khan and R. S. R. Gorla, "Heat and mass transfer in non-Newtonian nanofluids over a non-isothermal stretching wall," *Proc. Inst. Mech. Eng. Part N J. Nanoeng. Nanosyst.*, vol. 225, no. 4, pp. 155–163, 2011, doi: 10.1177/1740349912440680.
- [2] K. G. Kumar, B. J. Gireesha, B. C. Prasannakumara, and O. D. Makinde, "Impact of Chemical Reaction on Marangoni Boundary Layer Flow of a Casson Nano Liquid in the Presence of Uniform Heat Source Sink," *Diffus. Found.*, vol. 11, pp. 22–32, 2017, doi: 10.4028/www.scientific.net/df.11.22.
- [3] T. Hayat, S. A. Shehzad, and A. Alsaedi, "Soret and Dufour effects on magnetohydrodynamic (MHD) flow of Casson fluid," *Appl. Math. Mech. (English Ed.)*, vol. 33, no. 10, pp. 1301–1312, 2012, doi: 10.1007/s10483-012-1623-6.
- [4] D. A. Nield and A. Bejan, *Convection in porous media - Donald A.* 2006.
- [5] M. S. Malashetty, I. S. Shivakumara, and S. Kulkarni, "The onset of Lapwood-Brinkman convection using a thermal non-equilibrium model," *Int. J. Heat Mass Transf.*, vol. 48, no. 6, pp. 1155–1163, 2005, doi: 10.1016/j.ijheatmasstransfer.2004.09.027.
- [6] K. Sarada, R. J. P. Gowda, I. E. Sarris, R. N. Kumar, and B. C. Prasannakumara, "Effect of magnetohydrodynamics on heat transfer behaviour of a non-newtonian fluid flow over a stretching sheet under local thermal non-equilibrium condition," *Fluids*, vol. 6, no. 8, 2021, doi: 10.3390/fluids6080264.

- [7] D. Prakash, M. Muthtamilselvan, and X. D. Niu, "Unsteady MHD non-darcian flow over a vertical stretching plate embedded in a porous medium with thermal non-equilibrium model," *Adv. Appl. Math. Mech.*, vol. 8, no. 1, pp. 52–66, 2016, doi: 10.4208/aamm.2014.m462.
- [8] S. J. Kim and S. P. Jang, "Effects of the Darcy number, the Prandtl number, and the Reynolds number on local thermal non-equilibrium," *Int. J. Heat Mass Transf.*, vol. 45, no. 19, pp. 3885–3896, 2002, doi: 10.1016/S0017-9310(02)00109-6.
- [9] A. Alhadhrami *et al.*, "Numerical simulation of local thermal non-equilibrium effects on the flow and heat transfer of non-Newtonian Casson fluid in a porous media," *Case Stud. Therm. Eng.*, vol. 28, no. June, p. 101483, 2021, doi: 10.1016/j.csite.2021.101483.
- [10] M. Tencer, J. S. Moss, and T. Zapach, "Arrhenius average temperature: The effective temperature for non-fatigue wearout and long term reliability in variable thermal conditions and climates," *IEEE Trans. Components Packag. Technol.*, vol. 27, no. 3, pp. 602–607, 2004, doi: 10.1109/TCAPT.2004.831834.
- [11] A. R. Bestman, "Natural convection boundary layer with suction and mass transfer in a porous medium," *Int. J. Energy Res.*, vol. 14, no. 4, pp. 389–396, 1990, doi: 10.1002/er.4440140403.
- [12] K. A. Maleque, "Effects of exothermic/endothemic chemical reactions with arrhenius activation energy on MHD free convection and mass transfer flow in presence of thermal radiation," *J. Thermodyn.*, vol. 1, no. 1, 2013, doi: 10.1155/2013/692516.
- [13] M. I. Khan, T. Hayat, M. I. Khan, and A. Alsaedi, "Activation energy impact in nonlinear radiative stagnation point flow of Cross nanofluid," *Int. Commun. Heat Mass Transf.*, vol. 91, pp. 216–224, 2018, doi: 10.1016/j.icheatmasstransfer.2017.11.001.
- [14] A. V. Kuznetsov, "The onset of nanofluid bioconvection in a suspension containing both nanoparticles and gyrotactic microorganisms," *Int. Commun. Heat Mass Transf.*, vol. 37, no. 10, pp. 1421–1425, 2010, doi: 10.1016/j.icheatmasstransfer.2010.08.015.
- [15] A. V. Kuznetsov and A. A. Avramenko, "Effect of small particles on this stability of bioconvection in a suspension of gyrotactic microorganisms in a layer of finite depth," *Int. Commun. Heat Mass Transf.*, vol. 31, no. 1, pp. 1–10, 2004, doi: 10.1016/S0735-1933(03)00196-9.
- [16] M. Khan, M. Irfan, and W. A. Khan, "Impact of nonlinear thermal radiation and gyrotactic microorganisms on the Magneto-Burgers nanofluid," *Int. J. Mech. Sci.*, vol. 130, pp. 375–382, 2017, doi: 10.1016/j.ijmecsci.2017.06.030.

- [17] N. Begum, S. Siddiqa, and M. A. Hossain, "Nanofluid bioconvection with variable thermophysical properties," *J. Mol. Liq.*, vol. 231, pp. 325–332, 2017, doi: 10.1016/j.molliq.2017.02.016.
- [18] M. J. Uddin, Y. Alginahi, O. A. Bég, and M. N. Kabir, "Numerical solutions for gyrotactic bioconvection in nanofluid-saturated porous media with Stefan blowing and multiple slip effects," *Comput. Math. with Appl.*, vol. 72, no. 10, pp. 2562–2581, 2016, doi: 10.1016/j.camwa.2016.09.018.
- [19] Q. H. Shi *et al.*, "Numerical study of bio-convection flow of magneto-cross nanofluid containing gyrotactic microorganisms with activation energy," *Sci. Rep.*, vol. 11, no. 1, pp. 1–15, 2021, doi: 10.1038/s41598-021-95587-2.
- [20] H. Waqas, S. U. Khan, S. A. Shehzad, and M. Imran, "Radiative flow of Maxwell nanofluid containing gyrotactic microorganism and energy activation with convective Nield conditions," *Heat Transf. - Asian Res.*, vol. 48, no. 5, pp. 1663–1687, 2019, doi: 10.1002/htj.21451.